JOURNAL OF APPLIED POLYMER SCIENCE VOL. 16, PP. 3361–3373 (1972)

Melt Rheology of High-Density Polyethylene

MITSUYOSHI FUJIYAMA and YASUHIRO KAGIYAMA, *Research Laboratory, Tokuyama Soda Co., Ltd., Tokuyama-shi, Yamaguchi-ken, Japan*

Synopsis

The melt rheology of high density polyethylene was investigated. Linear viscoelasticity, capillary flow properties, and molecular weight parameter were measured with a plate relaxometer, capillary rheometer, and gel permeation chromatography, respectively. Intimate correlations among the slope of relaxation modulus curve, non-Newtonian flow behavior, Barus effect, and molecular weight parameter, $M_z(M_{z+1})/M_w$, respectively, were found.

INTRODUCTION

Many theoretical and experimental investigations have been reported about the relations between the molecular weight parameter of polymer melt and the linear viscoelasticity[1–13] and between the molecular weight parameter and non-Newtonian flow behavior.[13–28] There are several experimental investigations about the relations between the molecular weight parameter and the Barus effect[25,29–32] and between linear viscoelasticity and the non-Newtonian flow behavior.[33,34] However, little investigation has been done about the relations between linear viscoelasticity and Barus effect and between non-Newtonian flow behavior and Barus effect. Furthermore, the relations mentioned above are treated only between two properties and are not treated systematically among more than two properties.

In the present investigation, the melt rheology of high-density polyethylene was measured, and it was found that there were intimate correlations among the linear viscoelasticity, the capillary flow properties (non-Newtonian flow behavior, Barus effect), and the molecular weight parameter.

EXPERIMENTAL

Materials

Twenty-nine kinds of high-density polyethylenes, either commercial (A, B, C, and D) or polymerized experimentally by a low-pressure method (S), were used as samples. Their properties are shown in Table I.

TABLE I. Properties of Samples

Sample	Use	M_n	M_w	M_z	M_{z+1}	$\frac{M_z(M_{z+1})}{M_w}$	MI, (dg/min)	$\Delta \log t$	$\Delta H_{\dot{a}}$, (kcal/mole)	$\eta_{\tau=10^6}$, poise	$\frac{10^5}{\text{MI} \times \eta_{\tau=10^6}}$	$(D/D_0)_{\dot{\gamma}=10^2}$
A-1	Injection molding	1.42×10^4	6.67×10^4	1.99×10^5	4.15×10^5	1.24×10^6	14.0	0.70	5.5	2.44×10^3	2.92	1.40
A-2	Injection molding						6.5	0.80	6.2	4.33×10^3	3.56	1.45
A-3	Injection molding	1.36×10^4	7.62×10^4	2.05×10^5	3.68×10^5	9.98×10^5	6.0	0.80	5.7	5.24×10^3	3.19	1.50
A-4	Extrusion molding	2.04×10^4	1.06×10^5	4.70×10^5	1.30×10^6	5.76×10^6	0.9	1.16	6.0	2.13×10^4	5.21	1.77
A-5	Extrusion molding						0.5	1.18	5.7	4.14×10^4	4.84	1.75
A-6	Extrusion molding	2.15×10^4	1.86×10^5	1.31×10^6	2.71×10^6	1.91×10^7	0.2	1.75	7.1	4.26×10^4	11.71	1.87
A-7	Blow molding	1.36×10^4	8.72×10^4	4.54×10^5	1.21×10^6	6.28×10^6	0.8	1.43	6.0	2.09×10^4	5.98	1.98
A-8	Blow molding	1.44×10^4	1.39×10^5	7.79×10^5	1.55×10^6	8.67×10^6	0.3	1.78	5.1	3.54×10^4	9.41	1.86
A-9	Super-high MW						0.01					
B	Blow molding						0.50	1.37		4.48×10^4	7.05	1.54
C	Blow molding	2.22×10^4	1.25×10^5	6.93×10^5	2.48×10^6	1.37×10^7	0.32	1.47		3.34×10^4	8.30	1.64
D	Blow molding	1.61×10^4	1.87×10^5	8.18×10^5	1.45×10^6	3.58×10^6	0.17	1.29		3.83×10^4	15.35	1.58
S-1							17.9	0.98	6.0	1.27×10^3	4.40	1.70
S-2		1.42×10^4	8.53×10^4	3.18×10^5	7.90×10^5	2.95×10^6	6.5	0.87	6.4	4.35×10^3	3.54	1.44
S-3		1.50×10^4	1.01×10^5	4.01×10^5	9.98×10^5	3.96×10^6	2.5	0.95	6.0	1.09×10^4	3.67	1.58
S-4		1.87×10^4	1.52×10^5	7.03×10^5	1.74×10^6	8.04×10^6	0.90	1.10	5.5	2.97×10^4	3.74	1.66
S-5		1.50×10^4	1.01×10^5	4.01×10^5	9.98×10^5	3.96×10^6	0.19	1.08	6.7	9.10×10^4	5.79	1.55
S-6		1.47×10^4	8.83×10^4	3.37×10^5	8.38×10^5	3.20×10^6	5.40	0.86		4.08×10^3	4.54	1.62
S-7							1.28	1.76		7.64×10^3	10.21	1.85
S-8		1.05×10^4	8.26×10^4	4.17×10^5	1.05×10^6	5.30×10^6	1.08	1.25		1.67×10^4	5.55	1.81
S-9							0.94	1.43		1.67×10^4	6.38	1.92
S-10		2.16×10^4	1.34×10^5	4.13×10^5	9.00×10^5	2.77×10^6	0.81	1.04		2.56×10^4	4.82	1.67
S-11		0.95×10^4	1.35×10^5	9.70×10^5	1.96×10^6	1.41×10^7	0.77	1.43		2.33×10^4	5.60	1.81
S-12		1.37×10^4	1.31×10^5	9.33×10^5	2.18×10^6	1.55×10^7	0.63	1.32		2.86×10^4	5.55	1.76
S-13		1.81×10^4	1.88×10^5	1.05×10^6	1.95×10^6	1.09×10^7	0.54	1.57		2.63×10^4	7.05	1.88
S-14							0.48			2.44×10^4	8.55	1.73
S-15		1.89×10^4	1.60×10^5	7.11×10^5	1.43×10^6	6.37×10^6	0.41	1.38		3.00×10^4	8.12	1.68
S-16							0.40	1.54		2.98×10^4	8.39	1.76
S-17		1.86×10^4	2.31×10^5	1.34×10^6	2.45×10^6	1.42×10^7	0.33	1.85		2.63×10^4	11.51	1.74

Measurements

The molecular weight distributions were determined from gel permeation chromatography elution curves. A Waters Asssociates Model 200 chromatograph was used. Column packings were rigid polystyrene gel of pore size 10^6, 10^5, 10^4, and 10^3 Å.. The eluant was *ortho*-dichlorobenzene at 130°C.

Linear viscoelasticity was obtained by measuring the shear relaxation modulus $G(t)$ with a plate relaxometer. Details of the principle and the operation procedure are discussed elsewhere.[35] Measuring temperature was, as a rule, 190°C. For the samples A-1–A-8 and S-1–S-5, measurements were carried out at five temperatures, 150°, 170°, 190°, 210°, and 230°C, and then according to the time–temperature superposition principle,[1] the master curves of relaxation modulus reduced to 190°C were obtained.

The capillary flow properties were measured at 190°C with a Koka flow tester, a plunger extrusion-type rheometer produced by the Shimazu Seisakusho Co., Ltd., Japan. Its construction and usage have been described by Arai.[36] The die used was a flat die with the following dimension: capillary length $L = 5$ mm, capillary radius $R = 0.25$ mm, $L/R = 20$. The end correction for the shear stress and the non-Nestonian flow correction for the shear rate were not done, and only the apparent flow curve was obtained.

After the extrudate solidified, the diameter of the extrudate, D, was measured with a micrometer. The extrudate was not completely relaxed before measurement of diameter. The ratio D/D_0, where D_0 is the diameter of capillary, was defined as swelling ratio and was used as a measure of the Barus effect.

RESULTS AND DISCUSSION

Linear Viscoelasticity

The temperature variation of shear relaxation modulus $G(t)$ for sample A-6 is shown in Figure 1 as an example. According to the time–temperature superposition principle,[1] the master curve of the shear relaxation modulus reduced to 190°C was obtained and is shown in Figure 2. The master curves of the shear relaxation moduli for the A samples, obtained in the same way, are shown in Figure 3.

Sample A-9, which has a super-high molecular weight, shows a rubbery plateau in the measured time scale. From the viewpoint of processing method, the slope of the $G(t)$ curve is easier in the following order: blow molding grade (A-7, A-8) > extrusion molding grade (A-4, A-5) > injection molding grade (A-1, A-2, A-3). The temperature variation of the shift factor a_T, which was obtained from the time–temperature suerposition, obeyed the Arrhenius-type equation. The value of the apparent activation energy of relaxation, ΔH_a, is shown in Table I. The ΔH_a value of high-density polyethylene was about 6 kcal/mole.

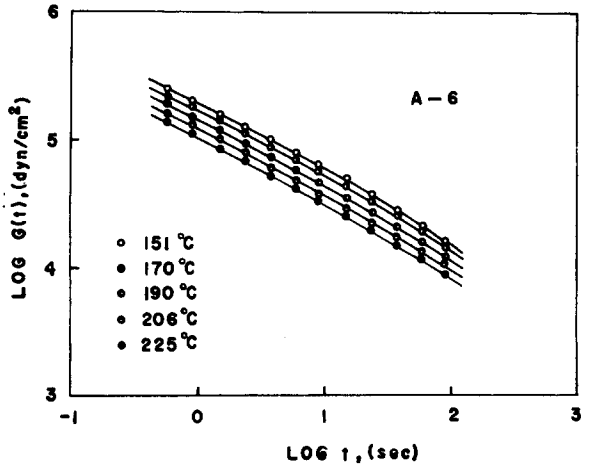

Fig. 1. Temperature variation of shear relaxation modulus for sample A-6.

The $\Delta \log t$ value, the time during which $\log G(t)$ value decreases from 5 to 4, may be employed as a measure of the slope of the $G(t)$ curve. As shown in Figure 4, $\Delta \log t$ correlates with the molecular weight parameter, $M_z(M_{z+1})/M_w$, as follows:

$$\log(\Delta \log t) \propto \log[M_z(M_{z+1})/M_w] \tag{1}$$

where M_w, M_z, and M_{z+1} are weight-, z-, and $(z + 1)$-average molecular weights, respectively. The symbol $\propto$ used in this paper means that there is a positive correlation between left side and right side.

The correlationship of eq. (1) is highly significant since the correlation coefficient $r_0 = 0.869$ and $r(18, 0.01) = 0.561$.

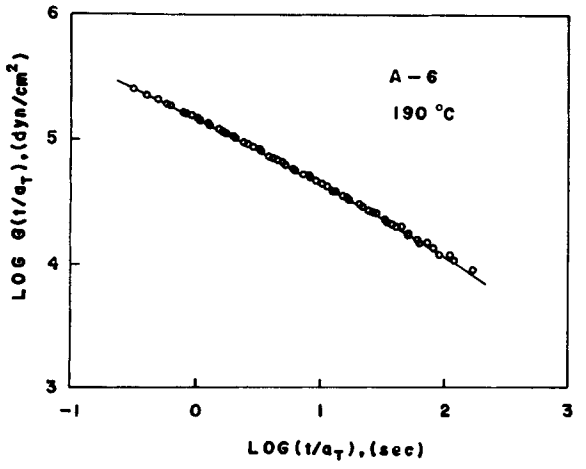

Fig. 2. Master curve of shear relaxation modulus reduced to 190°C for sample A-6.

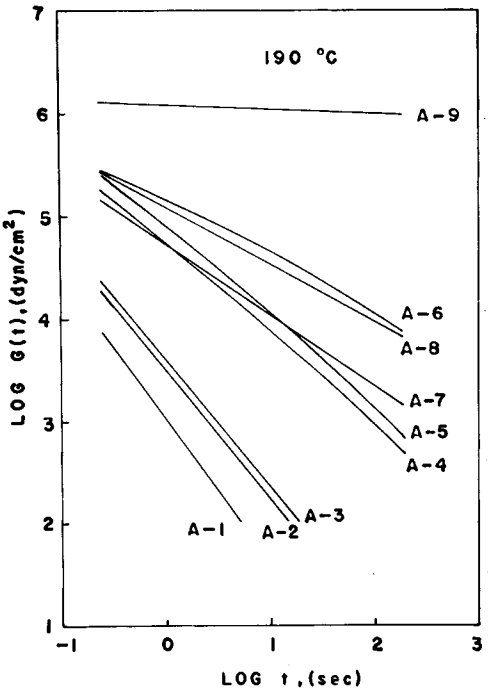

Fig. 3. Master curves of shear relaxation moduli for A samples.

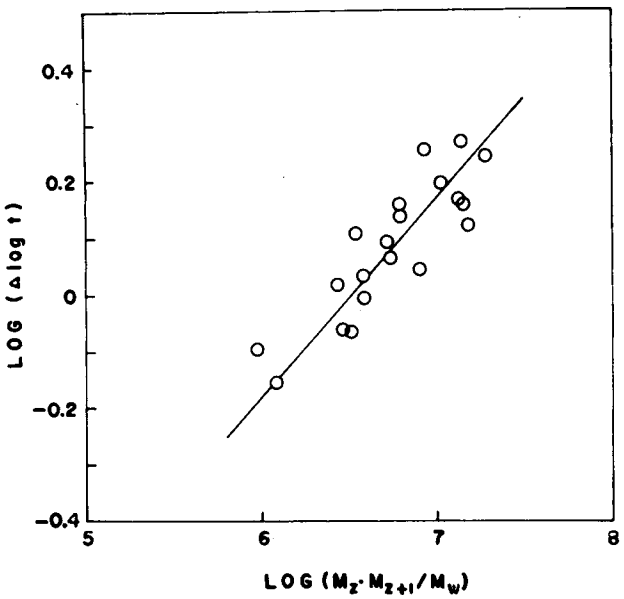

Fig. 4. Correlation between Δ log t, a measure of the slope of relaxation modulus curve, and molecular weight parameter, $M_z(M_{z+1})/M_w$. Correlation coefficient r_0 = 0.869**, $r(18, 0.01)$ = 0.561.

According to Ferry,[1] the steady-state shear compliance J_e^0 of polydisperse polymer is given by the equation (2):

$$J_e^0 = \frac{2}{5\rho RT} \cdot \frac{M_z(M_{z+1})}{M_w} \tag{2}$$

where ρ is the density of polymer melt, R is the gas constant, and T is the absolute temperature. Meanwhile, J_e^0 can be calculated from the $G(t)$ curve by eq. (3)[1]:

$$J_e^0 = \frac{\int_{-\infty}^{\infty} t^2 \cdot G(t) d\ln t}{\eta_0^2} = \frac{\int_{-\infty}^{\infty} t^2 \cdot G(t) d\ln t}{\left[\int_{-\infty}^{\infty} t \cdot G(t) d\ln t\right]^2} \tag{3}$$

where η_0 is the zero-shear viscosity. This equation shows that J_e^0 is governed mainly by the slope of the $G(t)$ curve. Accordingly, from eqs. (2) and (3) it can be well expected that there exists a correlation between $\Delta \log t$ which is a measure of the slope of the $G(t)$ curve and $M_z(M_{z+1})/M_w$.

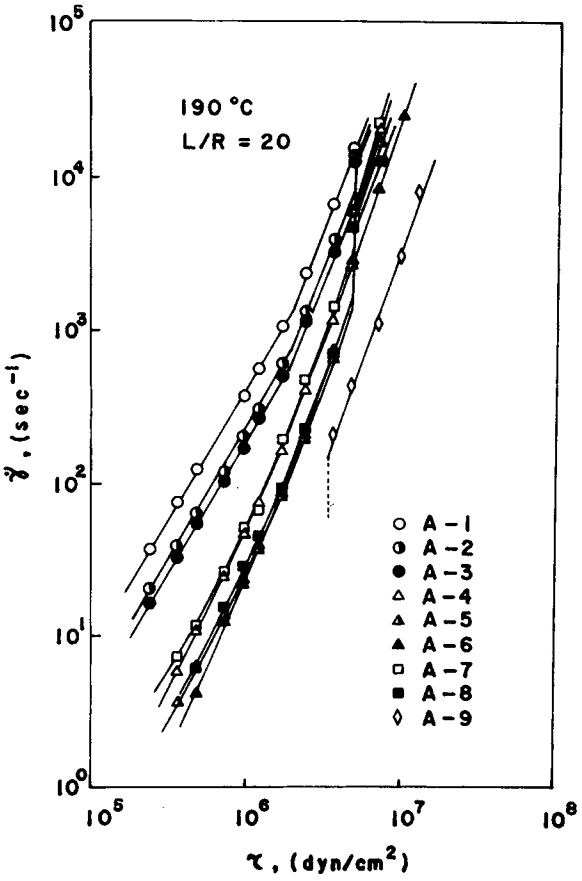

Fig. 5. Apparent flow curves for A samples.

From eq. (1), the slope of the $G(t)$ curve is assumed to be governed by a considerably high order of molecular weight and molecular weight distribution.

Non-Newtonian Flow

The apparent flow curves of the A samples are shown in Figure 5. The jumps in the flow curves are observed at a shear stress $\tau \doteqdot 5 \times 10^6$ dynes/cm^2. Sample A-9, which has a super-high molecular weight, does not flow below a definite shear stress and hence shows plastic flow behavior.

The values of the apparent viscosity at shear stress $\tau = 10^6$ dynes/cm^2, $\eta_{\tau=10^6}$, calculated from the apparent flow curves as shown in Figure 5, are shown in Table I. The reason why a value of 10^6 dynes/cm^2 was especially chosen as the shear stress is that the shear stress the polymer melt encounters when it is processed by extrusion molding and/or blow molding is about 10^6 dynes/cm^2.

The relation between $\eta_{\tau=10^6}$ and melt index (MI) is shown in Figure 6. From Figure 6 it is seen that eq. (4) holds:

$$\log \eta_{\tau=10^6} \propto -\log(MI). \tag{4}$$

The absolute value of the slope of the regression line is smaller than unity and the points scatter around the regression line. This fact derives from the differences of molecular weights and molecular weight distributions of the samples.

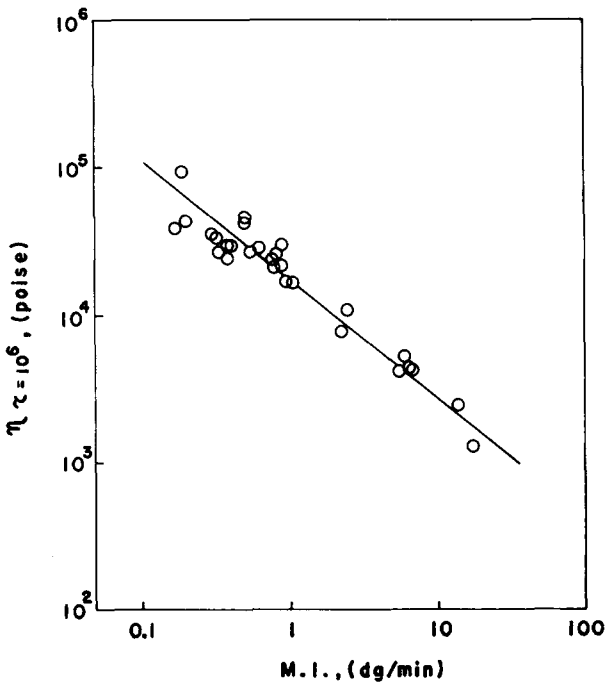

Fig. 6. Correlation between $\eta_{\tau=10^6}$, viscosity at shear stress $\tau = 10^6$ dynes/cm^2, and MI; $r_0 = -0.959^{**}$, $r(25, 0.01) = 0.487$.

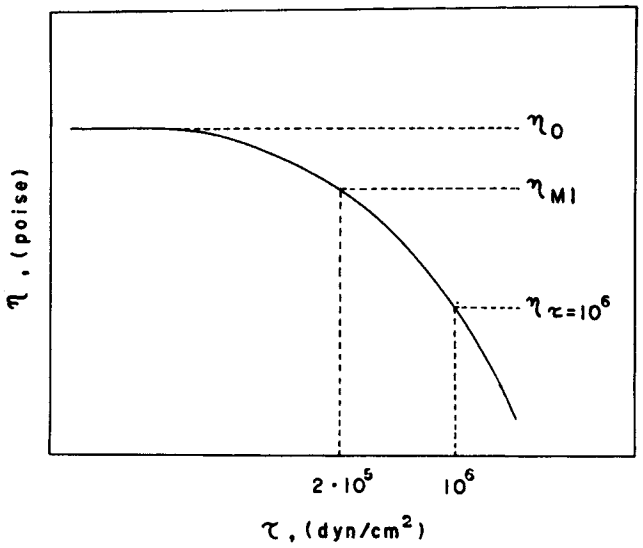

Fig. 7. Schematic representation for the variation of steady-flow viscosity η with shear stress τ.

The variation of steady-flow viscosity η with shear stress τ is schematically shown in Figure 7, where η_0 is the zero-shear viscosity, η_{MI} is the viscosity at the MI measurement, and $\eta_{\tau=10^6}$ is the viscosity at shear stress $\tau = 10^6$ dynes/cm^2.

Non-Newtonian index was defined by eq. (5),

$$\eta_{MI}/\eta_{\tau=10^6} \propto 1/MI \times \eta_{\tau=10^6} \tag{5}$$

and the non-Newton nature of the steady flow was represented numerically by it. The practical meaning of the non-Newtonian index is the index of fluidity at practical processing based on MI.

As shown in Figure 8, non-Newtonian index correlates with the molecular weight parameter, $M_z(M_{z+1})/M_w$, as follows:

$$\log(1/MI \times \eta_{\tau=10^6}) \propto \log[M_z(M_{z+1})/M_w]. \tag{6}$$

From eq. (6), the non-Newtonian index is assumed to be governed by considerably high order of molecular weight and molecular weight distribution.

As shown in Figure 9, the non-Newtonian index also correlates with $\Delta \log t$, which is a measure of the slope of the $G(t)$ curve, as follows:

$$\log(1/MI \times \eta_{\tau=10^6}) \propto \Delta \log t. \tag{7}$$

It is obvious from Figure 9 and eq. (7) that there is intimate correlation between the linear viscoelasticity ($\Delta \log t$) and the nonlinear steady flow property (non-Newtonian index).

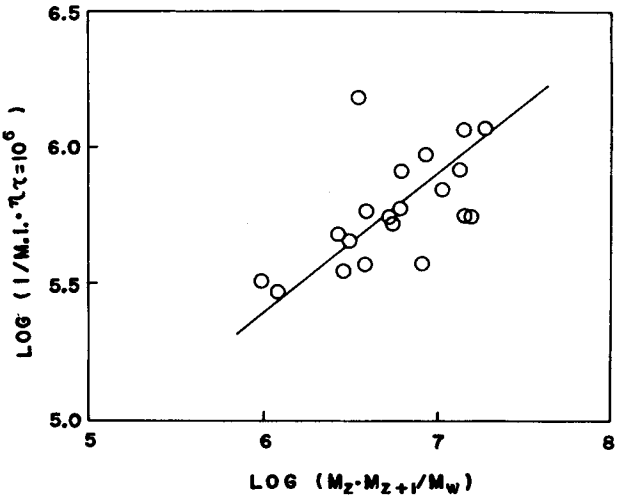

Fig. 8. Correlation between non-Newtonian index $1/MI \times \eta_{\tau=10^6}$ and $M_z(M_{z+1})/M_w$; $r_0 = 0.638^{**}$, $r(17, 0.01) = 0.575$.

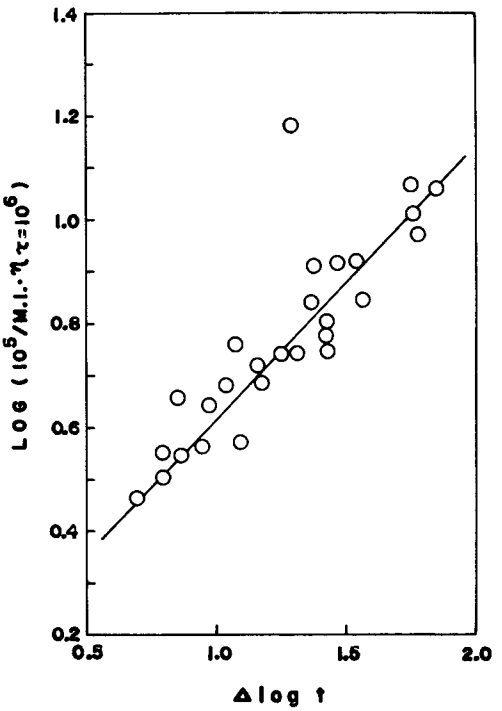

Fig. 9. Correlation between $1/MI \times \eta_{\tau=10^6}$ and $\Delta \log t$; $r_0 = 0.861^{**}$, $r(25, 0.01) = 0.487$.

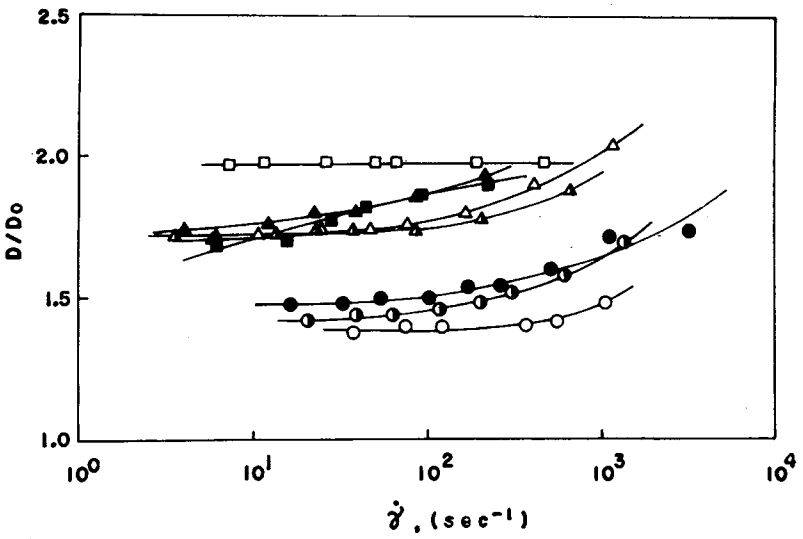

Fig. 10. Shear rate variation of swelling ratio D/D_0 for A samples. Symbols same as in Fig. 5.

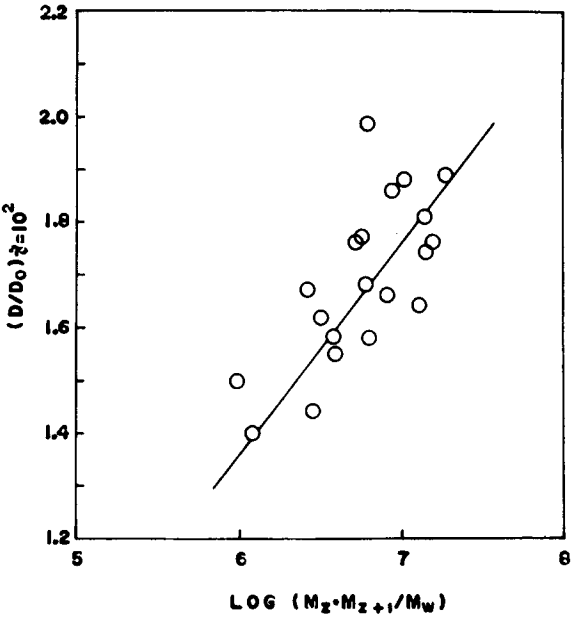

Fig. 11. Correlation between $(D/D_0)_{\dot{\gamma}=10^2}$, the swelling ratio at shear rate $\dot{\gamma} = 10^2\,\mathrm{sec}^{-1}$, and $M_z(M_{z+1})/M_w$; $r_0 = 0.718^{**}$, $r(18, 0.01) = 0.561$.

Barus Effect

The variation of swelling ratio D/D_0 with shear rate $\dot{\gamma}$ are shown for A samples in Figure 10. The symbols are the same as in Figure 5. From the viewpoint of processing methods, the Barus effect is more notable in the

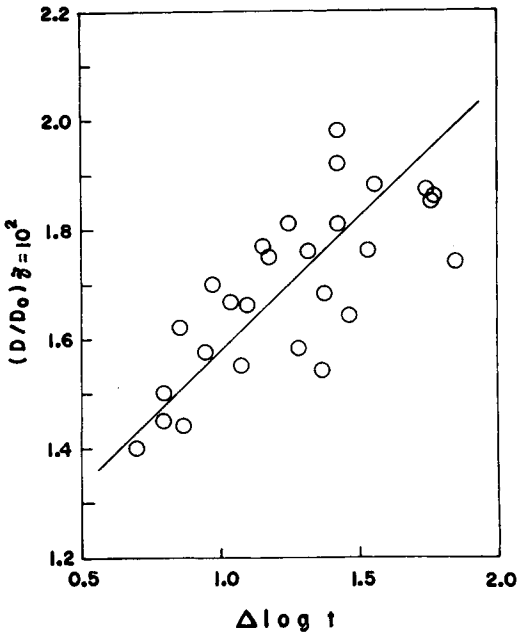

Fig. 12. Correlation between $(D/D_0)_{\dot{\gamma}=10^2}$ and $\Delta \log t$; $r_0 = 0.744^{**}$, $r(25, 0.01) = 0.487$.

following order: blow molding grade > extrusion molding grade > injection molding grade.

The swelling ratio at $\dot{\gamma} = 10^2$ sec^{-1}, $(D/D_0)_{\dot{\gamma}=10^2}$, may be used as a quantitative measure of the Barus effect. As shown in Figure 11, $(D/D_0)_{\dot{\gamma}=10^2}$ correlates with the molecular weight parameter, $M_z(M_{z+1})/M_w$, as follows:

$$(D/D_0)_{\dot{\gamma}=10^2} \propto \log[M_z(M_{z+1})/M_w]. \tag{8}$$

From this fact it is assumed that the Barus effect is governed by a considerably high order of molecular weight and molecular weight distribution.

Rogers[30] has shown that, although theoretically the notableness of the Barus effect correlates with $M_z(M_{z+1})/M_w$, in actual cases, it does not correlate with $M_z(M_{z+1})M_w$ but with M_w/M_n. Our experimental result did not agree with his experimental result but with his theoretical expectation.

As shown in Figure 12, $(D/D_0)_{\dot{\gamma}=10^2}$ correlates also with $\Delta \log t$ as follows:

$$(D/D_0)_{\dot{\gamma}=10^2} \propto \Delta \log t. \tag{9}$$

Furthermore, $(D/D_0)_{\dot{\gamma}=10^2}$ correlates also with non-Newtonian index as shown in Figure 13.

Although the swelling ratio at a shear rate $\dot{\gamma} = 10^2$ sec^{-1} was employed throughout this paper, the above correlations also exist for the swelling ratio at $\dot{\gamma} = 10^1$ sec^{-1}–10^3 sec^{-1}, which is the measured shear rate range.

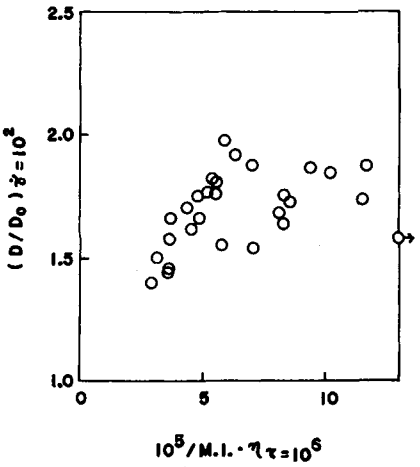

Fig. 13. Correlation between $(D/D_0)_{\dot{\gamma}=10^2}$ and $1/MI \times \eta_{\tau=10^6}$; $r_0 = 0.536^{**}$, $r(25, 0.01) = 0.487$.

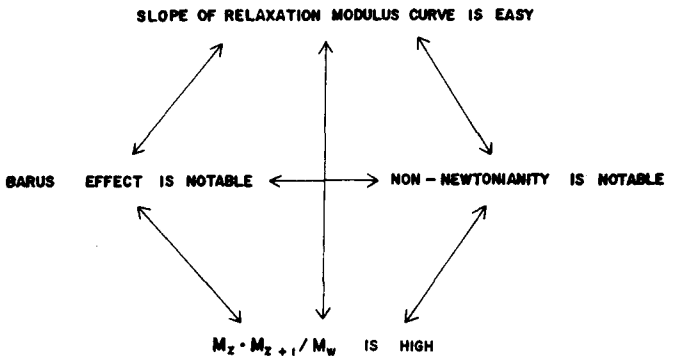

Fig. 14. Schematic representation for the correlationship among molecular weight parameter, linear viscoelasticity, and capillary flow properties.

CONCLUSION

As mentioned above, it became clear that intimate correlations exist among the molecular weight parameter $M_z(M_{z+1})/M_w$, the linear viscoelasticity $\Delta \log t$, and the capillary flow properties (non-Newtonian behavior, Barus effect), as shown in Figure 14. Of especial great interest are the intimate correlations between the linear viscoelasticity and the nonlinear steady flow properties.

The authors would like to thank Dr. K. Azuma for his encouragement during this work and Dr. H. Awaya for helpful discussions and cirticisms of the manuscript.

References

1. J. D. Ferry, *Viscoelastic Properties of Polymers*, Wiley, New York, 1960.
2. W. L. Peticolas, *J. Chem. Phys.*, **35**, 946 (1961).
3. W. L. Peticolas, *J. Chem. Phys.*, **39**, 3392 (1963).
4. G. Ajroldi and G. Pezzin, *Rheol. Acta*, **10**, 402 (1971).
5. G. P. Gluliani and A. De Chirico, *J. Macromol. Sci.-Phys.*, **B5**, 429 (1971).

6. K. Murakami, *Zairyo Shiken*, **10**, 367 (1961).
7. H. Fujita and K. Ninomiya, *J. Polym. Sci.*, **24**, 233 (1957).
8. K. Ninomiya and G. Yasuda, *Nippon Gomu Kyokaishi*, **39**, 168 (1966).
9. G. Yasuda, E. Maekawa, T. Honma, and K. Ninomiya, *Nippon Gomu Kyokaishi*, **39**, 177 (1966).
10. J. M. Watkins, R. D. Spangler, and E. C. McKannan, *J. Appl. Phys.*, **27**, 685 (1956).
11. V. A. Zosel, *Rheol. Acta*, **10**, 215 (1971).
12. W. M. Prest, Jr., *J. Polym. Sci. A-2*, **8**, 1897 (1970).
13. N. J. Mills, *Eur. Polym. J.*, **5**, 675 (1969).
14. W. W. Graessley, *J. Chem. Phys.*, **47**, 1942 (1967).
15. W. W. Graessley and L. Segal, *Macromolecules*, **2**, 49 (1969).
16. W. C. Uy and W. W. Graessley, *Macromolecules*, **4**, 458 (1971).
17. G. A. Toelcke, K. J. Modonia, C. G. Gogos, and J. A. Biesenberger, *Polym. Eng. Sci.*, **7**, 318 (1967).
18. R. N. Shroff and M. Shida, *Polym. Eng. Sci.*, **11**, 200 (1971).
19. H. L. Wagner and K. F. Wissbrun, *SPE Trans.*, 222, July (1962).
20. D. R. Mills, G. E. Moore, and D. W. Pugh, *SPE Trans.*, 40, January (1961).
21. S. Middleman, *J. Appl. Polym. Sci.*, **11**, 417 (1967).
22. N. Nakajima, *Proceeding of the Fifth International Congress on Rheology*, Vol. 4, 295 (1970).
23. C. K. Shih, *Trans. Soc. Rheol.*, **14**(1), 83 (1970).
24. R. Sabia, *J. Appl. Polym. Sci.*, **7**, 347 (1963).
25. J. E. Guillet, R. L. Combs, D. F. Slonaker, D. A. Weemes, and H. W. Coover, Jr., *J. Appl. Polym. Sci.*, **9**, 757 (1965).
26. M. M. Cross, *J. Appl. Polym. Sci.*, **13**, 765 (1969).
27. B. J. Cottam, *J. Appl. Polym. Sci.*, **9**, 1853 (1965).
28. N. Ishida, I. Shiga, and K. Sakamoto, *Kobunshi Kagaku*, **28**, 834 (1971).
29. R. W. Ford and J. D. Ilavsky, *J. Appl. Polym. Sci.*, **12**, 2299 (1968).
30. M. G. Rogers, *J. Appl. Polym. Sci.*, **14**, 1679 (1970).
31. I. Shiga, N. Ishida, J. Hashimoto, and K. Sakamoto, *Kobunshi Kagaku*, **28**, 839 (1971).
32. W. W. Graessley, S. D. Glasscock, and R. L. Grawley, *Trans. Soc. Rheol.*, **14**(4), 519 (1970).
33. M. Fujiyama and H. Awaya, *J. Appl. Polym. Sci.*, **16**, 275 (1972).
34. W. M. Prest, Jr., R. S. Porter, and J. M. O'Reilly, *J. Appl. Polym. Sci.*, **14**, 2697 (1970).
35. M. Fujiyama, S. Uemura, and M. Takayanagi, *Kogyo Kagaku Zasshi*, **71**, 540 (1968).
36. T. Arai, *A Guide to the Testing of the Rheological Properties of Koka Flow Tester*, Maruzen Co., Tokyo, 1958.

Received May 2, 1972
Revised June 21, 1972